Article

Synthesis of a Regioregular Zwitterionic Conjugated Oligoelectrolyte, Usable as an Optical Probe for Detection of Amyloid Fibril Formation at Acidic pH

Anna Herland, K. Peter R. Nilsson, Johan D. M. Olsson, Per Hammarstrm, Peter Konradsson, and Olle Ingans

J. Am. Chem. Soc., **2005**, 127 (7), 2317-2323• DOI: 10.1021/ja045835e • Publication Date (Web): 25 January 2005

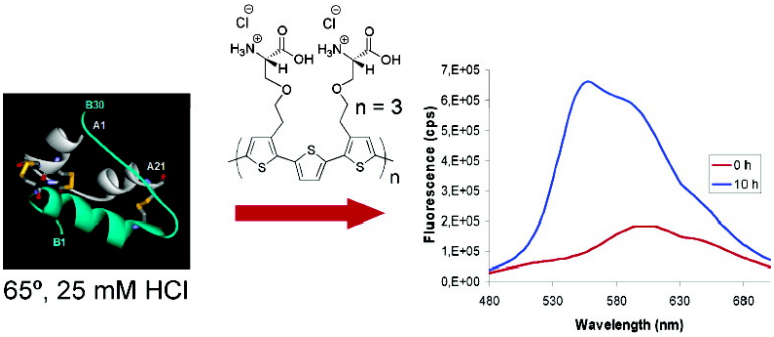

More About This Article

Additional resources and features associated with this article are available within the HTML version:

- Supporting Information
- Links to the 20 articles that cite this article, as of the time of this article download
- Access to high resolution figures
- Links to articles and content related to this article
- Copyright permission to reproduce figures and/or text from this article

View the Full Text HTML

J|A|C|S
ARTICLES
Published on Web 01/25/2005

Synthesis of a Regioregular Zwitterionic Conjugated Oligoelectrolyte, Usable as an Optical Probe for Detection of Amyloid Fibril Formation at Acidic pH

Anna Herland,[†] K. Peter R. Nilsson,[†] Johan D. M. Olsson,[‡] Per Hammarström,[‡] Peter Konradsson,*[,‡] and Olle Inganäs[†]

Contribution from the Department of Physics and Measurement Technology, Biology and Chemistry, Linköpings University, SE-581 83 Linköping, Sweden

Received July 12, 2004; E-mail: petko@ifm.liu.se

Abstract: Changes of the optical properties of conjugated polyelectrolytes have been utilized to monitor noncovalent interactions between biomolecules and the conjugated polyelectrolytes in sensor applications. A regioregular, zwitterionic conjugated oligoelectrolyte was synthesized in order to create a probe with a defined set of optical properties and hereby facilitate interpretation of biomolecule−oligoelectrolyte interactions. The synthesized oligoelectrolyte was used at acidic pH as a novel optical probe to detect amyloid fibril formation of bovine insulin and chicken lysozyme. Interaction of the probe with formed amyloid fibrils results in changes of the geometry and the electronic structure of the oligoelectrolyte chains, which were monitored with absorption and emission spectroscopy.

Introduction

Phenomenona such as misfolding and amyloid fibril formation are driving forces in the development of materials able to detect conformation changes in biomolecules. Conjugated polyelectrolytes have been used as probes for biomolecular interactions, through alternations of conditions for photoinduced charge transfer or excitation transfer[1−6] and through conformational changes of the polyelectrolyte chains.[7−9] Lately it has been shown that conjugated polymers (CPs) can be optical probes to monitor conformation changes of synthetic peptides[10,11] and calcium-induced conformation changes in calmodulin.[12] In photonic and electronic applications, oligomers have been used as model compounds for π-conjugated polymers.[13,14] Oligomers with a defined system offer the possibility to directly correlate physical properties with chemical structure. Series of well-defined π-conjugated oligomers have been studied in detail in order to correlate increasing chain length with changes in quantities such as optical adsorption maximum or oxidation potential.[13−16] Likewise, in biosensing applications where interactions between biomolecules and conjugated polyelectrolytes results in an alternation of the polymer backbone geometry, a change in absorption and emission characteristics of the polyelectrolyte would be observed. To facilitate the interpretation of the relation of such changes, it would be of great interest to use conjugated oligoelectrolytes in detection of biospecific interactions. Furthermore, a defined chain length makes detailed studies of the biomolecule/polyelectrolyte complex with X-ray crystallography and NMR an appealing task.

Folding of proteins to their functional, highly compact, native state is one of the most remarkable examples of biological self-assembly. However, under destabilizing conditions, proteins can aggregate into fibrillar assemblies, amyloid fibrils.[17,18] In addition to the loss of the original biological function of the protein, amyloid fibrils and the precursors thereof are being increasingly recognized as the cause of disease states, including Alzheimer's disease and spongiform encephalopathies.[17,19−23] Although no structural or sequential homology of amyloidogenic

[†] Department of Biomolecular and Organic Electronics.
[‡] Department of Chemistry.

(1) Wang, J.; Wang, D.; Miller, E. K.; Moses, D.; Bazan, G. C.; Heeger, A. J. *Macromolecules* **2000**, *33*, 5153−5158.
(2) Wang, D.; Gong, X.; Heeger, P. S.; Rininsland, F.; Bazan, G. C.; Heeger, A. J. *Proc. Natl. Acad. Sci. U.S.A.* **2002**, *99*, 49−53.
(3) Liu, B.; Gaylord, B. S.; Wang, S.; Bazan, G. C. *J. Am. Chem. Soc*. **2003**, *125*, 6705−6714.
(4) Heeger, P. S.; Heeger, A. J. *Proc. Natl. Acad. Sci. U.S.A.* **1999**, *96*, 12219−12221.
(5) Gaylord, B. S.; Heeger, A. J.; Bazan, G. C. *J. Am. Chem. Soc.* **2003**, *125*, 896−900.
(6) Gaylord, B. S.; Heeger, A. J.; Bazan, G. C. *Proc. Natl. Acad. Sci. U.S.A.* **2002**, *99*, 10954−10957.
(7) Ho, H.-A.; Boissinot, M.; Bergeron, M. G.; Corbeil, G.; Dore, K.; Boudreau, D.; Leclerc, M. *Angew Chem. Int. Ed.* **2002**, *41*, 1548−1551.
(8) Ho, H. A.; Leclerc, M. *J. Am. Chem. Soc.* **2004**, *126*, 1384−1387.
(9) Nilsson, K. P.; Inganas, O. *Nat. Mater*. **2003**, *2*, 419−424.
(10) Nilsson, K. P.; Rydberg, J.; Baltzer, L.; Inganas, O. *Proc. Natl. Acad. Sci. U.S.A.* **2003**, *100*, 10170−10174.
(11) Nilsson, K. P.; Rydberg, J.; Baltzer, L.; Inganas, O. *Proc. Natl. Acad. Sci. U.S.A.* **2004**, *101*, 11197−11202.
(12) Nilsson, K. P.; Inganäs, O. *Macromolecules* **2004**, *37*, 9109−9113.
(13) Martin, R. E.; Diederich, F. *Angew Chem. Int. Ed*. **1999**, *38*.
(14) Müllen, K.; Wegner, G. *Electronic materials: the oligomer approach*; Wiley-VCH: Weinheim, 1997.
(15) Meier, H.; Stalmach, U.; Kolshorn, H. *Acta Polym.* **1997**, *48*, 379−384.
(16) Frere, P.; Raimundo, J. M.; Blanchard, P.; Delaunay, J.; Richomme, P.; Sauvajol, J. L.; Orduna, J.; Garin, J.; Roncali, J. *J. Org. Chem.* **2003**, *68*, 7254−7265.
(17) Dobson, C. M. *Trends Biochem. Sci*. **1999**, *24*, 329−332.
(18) Sunde, M.; Serpell, L. C.; Bartlam, M.; Fraser, P. E.; Pepys, M. B.; Blake, C. C. *J. Mol. Biol.* **1997**, *273*, 729−739.
(19) Lansbury, P. T.; Kelly, J. W. *Amyloid* **1994**, *1*, 186−205.
(20) Sacchettini, J. C.; Kelly, J. W. *Nat. Rev. Drug Discov*. **2002**, *1*, 267−275.
(21) Dobson, C. M. *Nature* **2003**, *426*, 884−890.
(22) Carrell, R. W.; Lomas, D. A. *Lancet* **1997**, *350*, 134−138.
(23) Pepys, M. B. In *The Oxford Textbook of Medicine*, 3rd ed.; Weatherall, D. J., Ledingham, J. G. G., Warell, D. A., Eds.; Oxford University Press: Oxford, 1996; Vol. 2, pp 1512−1524.

Scheme 1. (i) NBS, $CHCl_3$/AcOH (1:1), 91 %; (ii) TsCl, Pyridine, $CHCl_3$, 87 %; (iii) N-*t*-Boc-L-Ser, K_2CO_3, DMF, 35 °C, 54 %; (iv) $Pd(OAc)_2$, KF, DMF, 31 %; (v) CH_2Cl_2/TFA (4:1), Quant.; (vi) $FeCl_3$, TBA-OTf, $CHCl_3$, 32 %

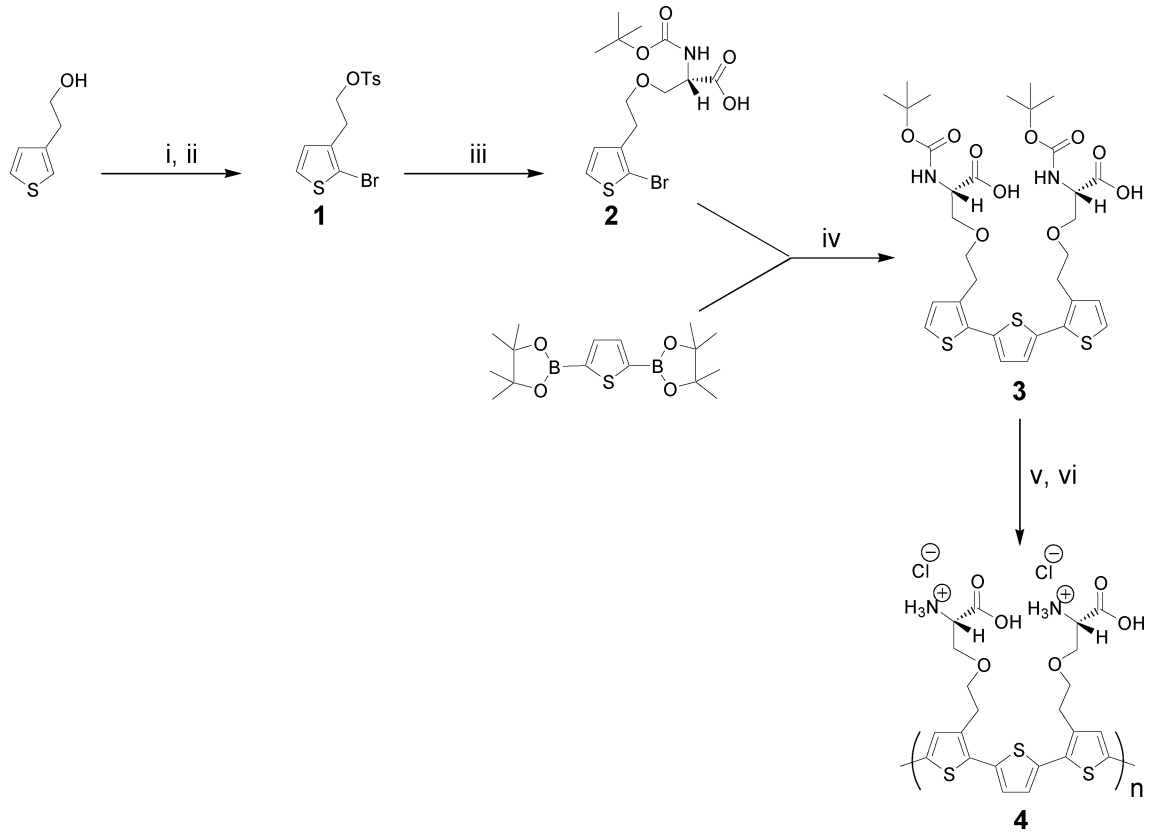

proteins, amyloid fibril structure appear generic showing linear filaments with a diameter of approximately 10 nm.[24] Fiber diffraction studies have revealed a cross-β structure as characteristic of amyloid fibrils, i.e., the β-strands are perpendicular to the fibril axes forming axially aligned extended β-sheets.[18]

Insulin, a 51-residue hormone, has a primarily helical native structure.[25] Insulin exists in equilibrium as a mixture of monomers, dimers, hexamers, and possibly higher-order oligomers, but the physically predominant form is a zinc-coordinated hexamer.[26] Insulin amyloid fibril formation is a well-studied phenomenon, which in vitro is known to occur at high protein concentrations, acidic pH, elevated temperatures, and exposure to hydrophobic surfaces.[27,28] Intermolecular hydrophobic forces have been suggested as the driving forces of the insulin fibril formation process.[29] Nielsen et al. have proposed a model for insulin fibril formation where dissociation of the native associated states (hexamer, tetramer, and dimer) into monomers is a prerequisite for fibrillation.[30] The monomer undergoes partial unfolding into an intermediate state, which oligomerizes to form the nucleus from which the amyloid fibrils grow.[26,30,31] Insulin fibril formation cause a variety of problems in handling soluble, therapeutic insulin.

Amyloid fibril formation of insulin has been studied with several spectroscopy and microscopy techniques[31−33] and through staining with small molecule dyes such as Congo Red and thioflavin T.[30,34] Herein we report the synthesis and optical characterization of a regioregular zwitterionic conjugated oligoelectrolyte, poly((3,3″-di[(*S*)-5-amino-5-carbonyl-3-oxapentyl]-[2,2′;5′,2″])-5,5″-terthiophenylene hydrochloride), PONT (Scheme 1), usable in a novel optical method to monitor amyloid fibril formation of bovine insulin and chicken lysozyme (CL) at acidic pH. The method is based on conformation changes of the conjugated oligoelectrolyte upon binding. The method has the advantage of being based on noncovalent assembly between the oligothiophene and the protein and the possibility to either add the probe after the amyloid fibril formation has occurred or with the probe present during the process.

Experimental Section

General Methods. Normal workup means drying the organic phase with $MgSO_4$(s) and filtration and evaporation of the solvent in vacuo at ∼45 °C. All dry solvents were collected onto 4-A predried molecular sieves (Merck). Thin-layer chromatography (TLC) was carried out on 0.25-mm precoated silica gel plates (Merck silica gel 60 F254), detected by UV absorption (254 nm) and/or by charring with PAA-dip (ethanol/sulfuric acid/*p*-anisaldehyde/acetic acid 90:3:2:1) followed by heating to ∼250 °C. FC means flash-column chromatography using silica gel

(24) Cohen, A. S.; Shirahama, T.; Skinner, M. In *Electron Microscopy of Protein*; Harris, I., Ed.; Academic Press: London, 1981; Vol. 3, pp 165−205.
(25) Blundell, T. L.; Cutfield, J. F.; Dodson, G. G.; Dodson, E.; Hodgkin, D. C.; Mercola, D. *Biochem. J.* **1971**, *125*, 50P−51P.
(26) Brange, J.; Andersen, L.; Laursen, E. D.; Meyn, G.; Rasmussen, E. *J. Pharm. Sci.* **1997**, *86*, 517−525.
(27) Waugh, D. F. *J. Am. Chem. Soc.* **1946**, *68*, 247−250.
(28) Nielsen, L.; Frokjaer, S.; Carpenter, J. F.; Brange, J. *J. Pharm. Sci.* **2001**, *90*, 29−37.
(29) Waugh, D. F.; Wilhelmson, D. F.; Commerford, S. L.; Sackler, M. L. *J. Am. Chem. Soc.* **1953**, *75*, 2592−2600.
(30) Nielsen, L.; Khurana, R.; Coats, A.; Frokjaer, S.; Brange, J.; Vyas, S.; Uversky, V. N.; Fink, A. L. *Biochemistry* **2001**, *40*, 6036−6046.
(31) Ahmad, A.; Millett, I. S.; Doniach, S.; Uversky, V. N.; Fink, A. L. *Biochemistry* **2003**, *42*, 11404−11416.
(32) Nettleton, E. J.; Tito, P.; Sunde, M.; Bouchard, M.; Dobson, C. M.; Robinson, C. V. *Biophys J.* **2000**, *79*, 1053−1065.
(33) Bouchard, M.; Zurdo, J.; Nettleton, E. J.; Dobson, C. M.; Robinson, C. V. *Protein Sci.* **2000**, *9*, 1960−1967.
(34) Glenner, G. G. *Prog. Histochem. Cytochem.* **1981**, *13*, 1−37.

(Merck 60 (0.040−0.063 mm)). ^{1}H and ^{13}C NMR spectra were performed on a Varian Mercury 300-MHz instrument at 25 °C. Chemical shifts are given in ppm relative to TMS in $CDCl_3$ (δ 0.00) for ^{1}H and ^{13}C or CD_3OD (δ 3.31) for ^{1}H and (δ 49.0) for ^{13}C NMR. Preparative high-performance liquid chromatography (HPLC) was performed on a Gynkotek (pump, P580; detector, UVD 170S; software, Chromeleon) using a Kromasil 100-10-C18 (250 × 20 mm) column. Optical rotations were recorded at room temperature with a Perkin-Elmer 141 polarimeter; IR spectra were recorded on a Perkin-Elmer SPECTRUM 1000 FT-IR spectrometer as KBr pellets and melting points were recorded with a Gallenkampmelting point apparatus.

Synthesis of 2-(2-Bromo-3-thienyl)-*p*-toluenesulfonyl ethanol (1). 2-(3-Thienyl)ethanol (3.75 mL, 33.34 mmol) was dissolved in $CHCl_3$/AcOH (1:1, 90 mL) and cooled to 0 °C. N-Bromosuccinimide (6.26 g, 35.17 mmol) was added to the solution, and after 30 min, the solution was diluted with H_2O (250 mL). The organic layer was washed with 10% KOH (aq) (2 × 70 mL) and H_2O (2 × 70 mL) and subjected to normal workup. FC (T/E 4:1) gave the 2-bromosubstituted product (6.30 g, 30.40 mmol, 91%) as an oil (R_f = 0.43 (toluene/EtOAc 4:1)). The brominated product (3.21 g, 15.48 mmol) was dissolved in $CHCl_3$ (60 mL) and cooled to 0 °C; pyridine (2.49 mL, 30.5 mmol) and *p*-toluenesulfonyl chloride (4.43 g, 23.24 mmol) were added. After 24 h, the reaction was quenched by adding H_2O (20 mL) and diluted with Et_2O (100 mL). The organic layer was washed with 2 M HCl (2 × 40 mL), sat. $NaHCO_3$ (aq.) (2 × 40 mL), and H_2O (2 × 40 mL) and subjected to normal workup. FC (toluene) and crystallization from EtOAc/hexane afforded **1** (4.89 g, 13.54 mmol, 87%) as white needles. R_f = 0.64 (toluene/EtOAc 4:1). M

p: 38−39 °C (from EtOAc/hexane).

IR ν_{max} cm^{-1}: 552, 663, 713, 773, 902, 971, 1171, 1186, 1359, 1595.

^{13}C NMR ($CDCl_3$) δ: 21.9, 29.4, 68.9, 111.1, 126.1, 128.0 (2C), 128.7, 130.1 (2C), 133.1, 135.9, 145.0.

^{1}H NMR ($CDCl_3$) δ: 2.43 (s, 1H), 2.93 (t, 2H, J = 6.9 Hz), 4.17 (t, 2H, J = 6.9 Hz), 6.76 (d, 1H, J = 6.0 Hz), 7.17 (d, 1H, J = 6.0 Hz), 7.30 (d, 2H, J = 8.3 Hz), 7.71 (d, 2H, J = 8.3 Hz).

Anal. Calcd for $C_{13}H_{13}BrO_3S_2$: C, 43.2; H, 3.6; S, 17.8. Found: C, 43.4; H, 3.8; S, 17.5.

Synthesis of (*S*)-3-[2-(2-Bromo-3-thienyl)-ethoxy]-2-*tert*-butoxy-carbonylamino-propionic acid (2). N-*t*-Boc-L-Ser (3.04 g, 14.80 mmol) and **1** (2.97 g, 8.22 mmol) were dissolved in dry DMF (150 mL) under N_2 atmosphere. K_2CO_3 (3.41 g, 24.66 mmol) was added, and the solution was heated to 35 °C. After 30 h, H_2O (100 mL) was added, and the mixture was poured over cold 2 M HCl (100 mL) and washed with toluene (3 × 100 mL). The organic layer was washed with H_2O (80 mL), subjected to normal workup, and purified by FC (toluene/EtOAc 4:1) to give **2** (1.75 g, 4.44 mmol, 54%) as a colorless syrup. R_f = 0.54 (toluene/EtOAc 1:1).

$[\alpha]_D$ = −4.9 (*c* 2.0, $CHCl_3$).

IR ν_{max} cm^{-1}: 641, 723, 1061, 1164, 1367, 1510, 1711, 2977, 3430.

^{13}C NMR ($CDCl_3$) δ: 28.5 (3C), 28.9, 56.0, 62.9, 64.5, 80.3, 110.7, 126.1, 128.6, 137.1, 156.1, 171.1.

^{1}H NMR ($CDCl_3$) δ: 1.45 (s, 9H), 2.96 (t, 2H, J = 6.8 Hz), 3.81 (dd, 1H, J = 3.5, 11.1 Hz), 3.91 (dd, 1H, J = 3.5, 11.1 Hz), 4.35 (m, 3H), 6.85 (d, 1H, J = 5.6 Hz), 7.23 (d, 1H, J = 5.6 Hz).

Anal. Calcd for $C_{14}H_{20}BrNO_5S$: C, 42.7; H, 5.1; S, 8.1. Found: C, 42.7; H, 5.2; S, 8.1.

Synthesis of 3,3″-di[(*S*)-5-*tert*-Butoxycarbonylamino-5-carbonyl-3-oxapentyl]-2,2′;5′,2″-terthiophene (3). Compound **2** (0.195 g, 0.49 mmol), thiophene-2,5-bis-pinacolboronate[35] (0.080 g, 0.24 mmol), KF (0.083 g, 1.428 mmol), and $Pd(OAc)_2$ (0.005 g, 0.024 mmol) were added to an oven-dried flask. After a flush with Ar, dry DMF (3 mL) was added. After the solution was stirred for 6 h in an Ar atmosphere, the mixture was diluted with H_2O (15 mL) and washed with toluene (5 × 15 mL). The organic layer was subjected to normal workup, FC (toluene/EtOAc 1:1), and HPLC (MeOH/H_2O 80:20 + 0.2% TFA) to give **4** (0.053 g, 0.074 mmol, 31%) as an oil. R_f = 0.60 (toluene/EtOAc 1:3).

$[\alpha]_D$ = −18.3 (*c* 2.0, $CHCl_3$).

IR ν_{max} cm^{-1}: 801, 835, 1060, 1367, 1506, 1713, 2975, 3107, 3399.

^{13}C NMR ($CDCl_3$) δ: 28.3 (6C), 28.4 (2C), 55.8 (2C), 63.5 (2C), 65.1 (2C), 80.3 (2C), 124.8 (2C), 127.0 (2C), 129.8 (2C), 132.2 (2C), 134.0 (2C), 135.6 (2C), 155.5 (2C), 170.8 (2C).

^{1}H NMR ($CDCl_3$) δ: 1.44 (s, 18 H), 3.19 (t, 4H, J = 7.0 Hz), 3.82 (dd, 2H, J = 3.6, 11.1 Hz), 3.88 (dd, 2H, J = 3.6, 11.1 Hz), 4.42 (m, 6H), 6.98 (d, 2H, J = 5.1 Hz), 7.11 (s, 2H), 7.24 (d, 2H, J = 5.1 Hz).

Anal. Calcd for $C_{32}H_{42}N_2O_{10}S_3Br$: C, 54.1; H, 6.0; S, 13.5. Found: C, 54.0; H, 6.2; S, 13.6.

Synthesis of PONT (4). Compound **3** (37 mg, 0.052 mmol) was dissolved in CH_2Cl_2/TFA (4:1, 2 mL). The reaction was quenched after 1 h by adding MeOH (1 mL) and co-concentrated with toluene (3 × 3 mL). The ammonium salt and TBA-OTf (52 mg, 0.13 mmol) were dissolved in dry $CHCl_3$ (1.5 mL), and the solution was cooled to 0 °C. Anhydrous $FeCl_3$ (37 mg, 0.23 mmol) was added to this solution under an Ar atmosphere. After the solution was stirred for 10 h at room temperature, the reaction was quenched with H_2O (2 mL) and diluted with $CHCl_3$ (3 mL). The organic layer was washed with H_2O (3 × 2 mL). The aqueous solution was diluted with acetone (25 mL), and concentrated HCl was added dropwise until the polymer precipitated. After 2 h, the mixture was centrifuged (4 min/2500 rpm), and the red salt was washed with acetone twice, dissolved in H_2O (2.5 mL), and reprecipitated from acetone/concentrated HCl. The washing procedure was repeated twice to give **4** (10 mg, 0.017 mmol, 32%) as a dark red powder.

IR ν_{max} cm^{-1}: 793, 821, 1061, 1229, 1503, 1741, 2952, 3190.

^{1}H NMR (CD_3OD) δ: 3.26 (s) (peak partly hidden in MeOH (δ: 3.31), 3.97 (s, 12H), 4.16 (s, 14H), 4.56 (s, 12H), 7.12 (d, 2H, J = 5.5 Hz), 7.23 (s, 4H), 7.31 (s, 6H), 7.42 (d, 2H, J = 5.5 Hz).

Protein Preparation. Bovine insulin was obtained from Sigma-Aldrich. The lyophilized protein was dissolved in 2 M guanidine hydrochloride and was dialyzed vs three rounds of 25 mM HCl at 4 °C. The insulin solutions (0.5−2.0 mM) were stored at 4 °C and were stable for several weeks. Lyophilized lysozyme from hen egg white was obtained from Sigma and was dissolved in dH_2O at a concentration of 0.7 mM. The protein was dialyzed vs three rounds of 25 mM HCl at 4 °C or vs 10 mM Na phosphate buffer, pH 7.5. Filtered (0.45 μm) stock solutions were made at concentrations of 0.61 mM. Collagen from rabbit, type I, acid soluble was obtained from Sigma and dissolved in 0.5 M acetic acid at a concentration of 5 mg/mL.

Amyloid Fibril Formation. A stock solution containing 320 μM bovine insulin in 25 mM HCl was prepared. A solution containing 320 μM bovine insulin and 390 μM PONT (on a 9-monomer basis) in 25 mM HCl was prepared. The solutions were placed in a water bath with a temperature of 65 °C to induce the amyloid formation. Samples were taken and analyzed during a time period of 3 days. Lysozyme fibrils were made through incubation of the protein in 25 mM HCl at 65 °C for 220 h.

Transmission Electron Microscopy (TEM) Experiments. Aliquots collected at different time points during fibril formation were diluted in 25 mM HCl and applied to carbon-coated grids for 2 min. The grids were washed and negatively stained with uranyl acetate 2% (wt/vol) in water and air dried before being examined in a Phillips EM400 transmission electron microscope at an accelerating voltage of 120 kV.

Optical Measurements. Stock solutions containing 1.5 mg mL^{-1} PONT in deionized water was prepared. The oligoelectrolyte solution (10 μL) was diluted with deionized water or the buffer in question, 25 mM HCl, 20 mM MES pH 5.9, and 20 mM Na carbonate pH 10, to a final volume of 1500 μL. In the samples where insulin/lysozyme fibril formation was studied, 10 μL of the oligoelectrolyte solution was mixed with aliquots of protein samples taken at different time points of

(35) Parakka, J. P.; Jeevarajan, J. A.; Jeevarajan, A. S.; Kispert, L. D.; Cava, M. P. *Adv. Mater.* **1996**, *8*, 54−59.

incubation under fibril formation conditions, i.e., 25 μL of the bovine insulin solution (25 mM HCl) or 13.1 μL of the chicken lysozyme solution (25 mM HCl), and diluted with 25 mM HCl to a final volume of 1500 μL containing 5 μM insulin/ lysozyme. In the samples where collagen was studied, 50 μL of the collagen solution (0.5 M acetic acid) was mixed with 50 μL 20 mM Na acetate pH 4.2, 6.7 μL of the oligoelectrolyte solution was added, and the sample was diluted in 25 mM HCl to a final concentration of 1000 μL.

In the samples where PONT were present during the amyloid fibril formation, 25 μL of the bovine insulin and PONT solution was diluted with 25 mM HCl to a final volume of 1500 μL. The samples were incubated for 5 min at room temperature, and the emission spectra were recorded with an ISA Jobin-Yvon spex FluoroMax-2 apparatus. A Perkin-Elmer Lambda 9 UV/VIS/NIR spectrophotometer was used for the absorption measurements, and the circular dichroism (CD) spectra were recorded with an ISA Jobin-Yvon CD6 (5-mm quartz cell).

Results and Discussion

Synthesis of PONT. 2-(3-Thienyl)ethanol was brominated with NBS and tosylated into derivative **1**. The tosyl group was displaced by a Boc-protected amino acid, N-*t*-Boc-Ser, to afford **2**. Palladium-catalyzed cross coupling of **2** and thiophene-2,5-bispinacolboronate[35] gave a regioregular terthiophene, **3**, in acceptable yield. The Suzuki-type coupling turned out to be crucial. Several Pd reagents, both with different ligands as well as "ligandsless" $Pd(OAc)_2$, and bases were tried under different conditions (solvent, temperature, etc.). The choice of activator, base, and solvent proved to be essential for reaction. Using $Pd(OAc)_2$ with KF as base in DMF gave the best yield of compound **3**. The low yield of product was partly explained by hydrolytic deboronation to a monosubstituted thiophenedimer, an earlier detected problem in palladium-catalyzed coupling of electron-rich systems.[36] The Boc groups were removed in CH_2Cl_2/TFA to give the corresponding ammonium salt readily for polymerization. Because of the functional groups of the terthiophene, the polymerization was performed by a method reported by Sugimoto et al.[37,38] using chemical oxidation with anhydrous $FeCl_3$ in $CHCl_3$. The water-soluble oligomer was then precipitated by adding acetone and concentrated hydrochloric acid, washed with acetone, and dried to achieve **4** as a red powder (Scheme 1).

Matrix Assisted Laser Desorption/Ionization Time-of-Flight Mass Spectroscopy (MALDI-TOF-MS). The length of the regioregular thiophene backbone in the oligomer was further elucidated by MALDI-TOF-MS. An aqueous solution (1 μL) of the oligomer and 1 μL of the matrix (α-cyano-4-hydroxy-*trans*-cinnamic acid (CHCA) in 0.1% TFA/acetonitrile (1:1)) were coevaporated on a target plate, and the spectra were recorded in linear positive mode. The MALDI-TOF spectra of the product obtained from polymerization of the terthiophene **3** with $FeCl_3$ in $CHCl_3$ in the presence of TBA-OTf gave a major peak with a mass of 1529 (Figure 1). This peak corresponds to an oligomer containing nine thiophene rings in the backbone (Scheme 1). Minor traces of peaks with masses of 2037 (less than 15% intensity) and 2546 (less than 5% intensity) were also found in the spectra, these peaks correspond to oligomers of 12 and 15 thiophene units in the backbone, respectively.

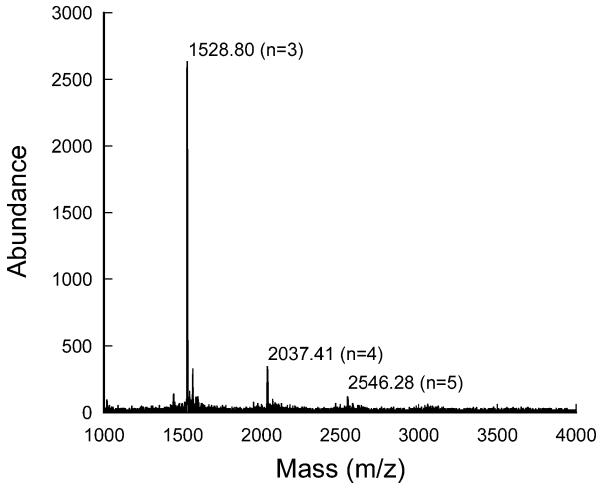

Figure 1. MALDI-TOF-MS spectra of PONT recorded in a linear positive mode using CHCA as matrix.

CD Measurements. Amyloid fibril formation at low pH and elevated temperature has previously been studied with CD.[31,33] Native BI (nBI) in 25 mM HCl shows a characteristic α-helical spectrum (see Supporting Information, Figure S1) in the far UV region, with strong negative peaks at 208 and 222 nm, which is consistent with the crystal structure of the insulin hexamer.[18] Fibrillation in BI at 65 °C (320 μM, in 25 mM HCl) was followed by CD over a period of 10 h, when a β-sheet-rich structure was obtained (see Supporting Information, Figure S1). This conversion of the BI from an α-helical-rich to a more β-sheet-rich structure is a clear indication of amyloid fibril formation of the protein. Our results are in good agreement with an earlier CD and FTIR study of the amyloid formation in BI,[33] although the concentration of BI was much higher in that study than the concentration used herein. CD spectra of nBI/PONT solutions (data not shown) were very similar to the results for the pure nBI solutions, showing that the interaction between PONT and BI has no major impact on the secondary structure of nBI.

TEM Measurements. The conditions, acidic pH and elevated temperature, used in this procedure are highly favorable for aggregation and fibril formation.[27] The electron micrograph taken after 2 h after the initiation of heating show spherical aggregates (Figure 2a), which is consistent with studies made under similar solution conditions.[26,32,33] Figure 2b shows an electron micrograph of the sample heated for 3.5 h. A few fibrils can clearly be seen, but there are also numerous spherical aggregates. In the period of 4−10 h, a network of fibrils appears followed by a decrease of aggregates. After 10 h, both smooth fibrils with curvature, indicative of flexibility, and more mature twisted fibrils with an average width of 7−10 nm can be seen. The amount of spherical aggregates has substantially declined. The EM studies agree very well with the lag phase (0−4 h incubation), the exponential growth phase (4−7 h), and the plateau phase (from 7 h) observed in a study where the amyloid formation of BI was monitored by Congo red and an anionic conjugated polythiophene.[39]

Optical Characterization of PONT. The absorption spectra of PONT at different pH and in deionized water are shown in Figure 3. The oligoelectrolyte undergoes a pH-induced orange

(36) Martina, S.; Enkelmann, V.; Schlueter, A. D.; Wegner, G. *Synth. Metals* **1991**, *41*, 403−406.
(37) Sugimoto, R.; Takeda, S.; Gu, H. B.; Yoshino, K. *Chem. Exp.* **1986**, *1*, 635.
(38) Yoshino, K.; Hayash, S.; Sugimoto, R.-I. *Jpn. J. Appl. Phys.* **1984**, *23*, L899.
(39) Nilsson, K. P.; Herland, A.; Hammarström, P.; Inganäs, O. *Biochemistry* **2005**, in press.

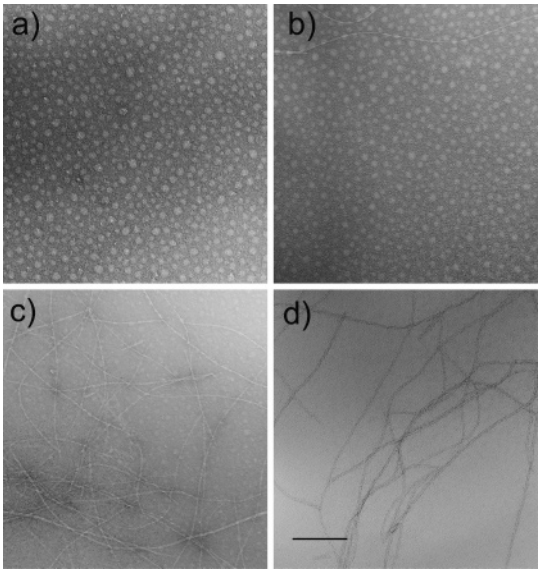

Figure 2. (a) 2-h incubation. (b) 3.5-h incubation. (c) 6-h incubation. (d) 10-h incubation. The scale bar represents 200 nm.

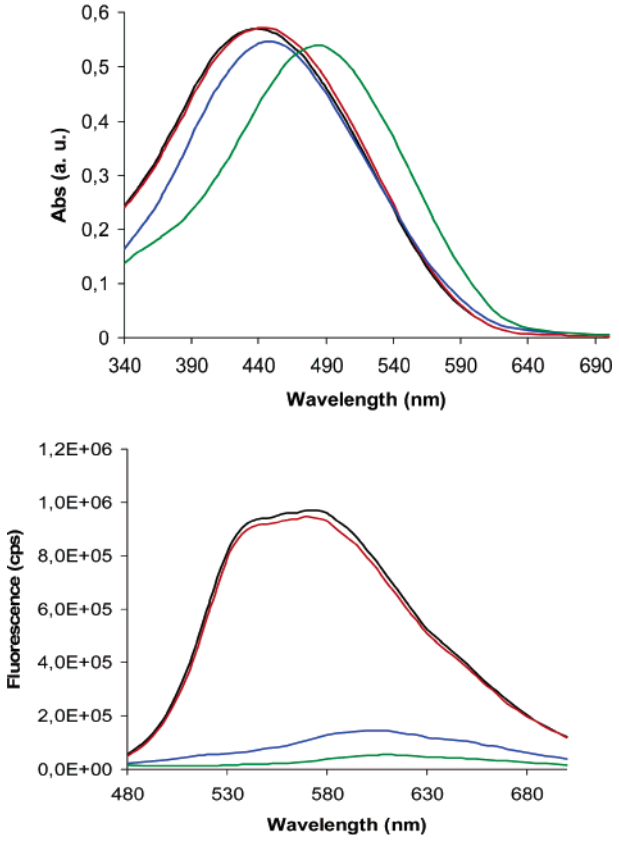

Figure 3. Absorption spectra (top) and emission spectra (bottom) of PONT after 10 min of incubation in deionized water (black), pH 1.6 (blue), pH 5.9 (red), and pH 10 (green). All the emission spectra were recorded with excitation at 400 nm.

to red color (a shift of the absorption maximum from 434 to 484 nm) alteration, indicating that deprotonation and protonation of the amino and the carboxyl groups have an influence on the coil-to-rod (nonplanar to planar) conformation transition of the oligoelectrolyte backbone. The nonplanar conformation seems to be most abundant at pH 5.9 (pK_a for serine) and in deionized water. As the side chains become charged, either positively or negatively, the oligoelectrolyte chains adopt a more planar

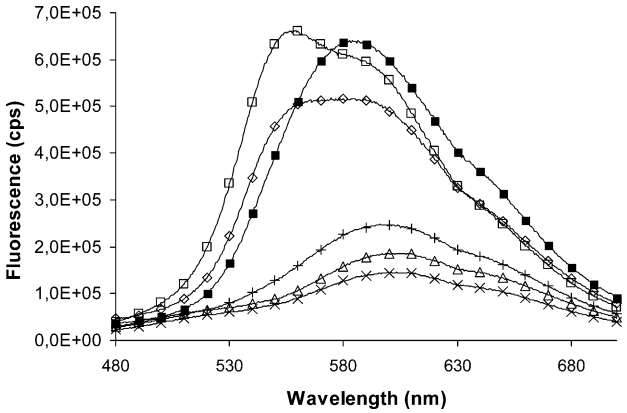

Figure 4. Emission spectra of 6.5 μM PONT−HCl (on a chain basis) in 25 mM HCl (×), 25 mM HCl with 5.0 μM of nBI (△), 25 mM HCl with 5.0 μM fBI after 4.5 h in 65 °C (+), 25 mM HCl with 5.0 μM fBI after 6 h in 65 °C (◊), and 25 mM HCl with 5.0 μM fBI after 10 h in 65 °C (□). An aliquot was withdrawn, and after addition of PONT, the samples were diluted with 25 mM HCl (23 °C) prior to emission measurements. Emission spectra of 6.5 μM PONT−HCl (on a chain basis) present during heat incubation in 25 mM HCl with 5.0 μM fBI after 10 h in 65 °C (■). The emission spectra were recorded with excitation at 400 nm.

conformation, observed as a red shift of the absorption maximum. Interestingly, the planarization of the backbone is more significant at alkaline pH, indicating that the oligoelectrolyte backbone adopts different conformations in acidic and alkaline environment. The oligoelectrolyte is probably adopting the extended rod-shaped conformation due to electrostatic repulsion forces between the oligoelectrolyte side chains,[40,41] or hydrogen bonding[42] and hydrophobic assembly between nearby PONT chains, as these molecular forces are highly influenced by the charge of the oligoelectrolyte side chains.

The pH-induced conformational changes of the oligoelectrolyte chains will also alter the emission spectra for the oligoelectrolyte solutions (Figure 3). At pH = 5.9 (pI for serine) and in deionized water, light with a shorter wavelength is emitted and the emission maximum is approximately 555 nm. Interestingly, as the net charge of the oligoelectrolyte side chains become more negative or positive, PONT emits light with a decreased intensity and longer wavelengths. At pH 10, the oligoelectrolyte emits light with a wavelength around 615 nm, and in 25 mM HCl (pH 1.6), an emission maximum of 600 nm is seen (Figure 3), indicating that the deprotonation and protonation of the amino and the carboxyl groups are inducing a planarization of the oligoelectrolyte backbone and aggregation of oligoelectrolyte chains. Similar results have been seen for a zwitterionic conjugated polyelectrolyte, POWT, and the decreased intensity of the emitted light is due to de-excitation events created by contact between polymer chains.[43,44]

Detection of Amyloid Fibril Formation. Upon addition of 5 μM nBI (pH 1.6) to PONT, the emission maximum remains at 600 nm (Figure 4), but the intensity of the emission has slightly increased, suggesting that a minor separation of poly-

(40) Kim, B.; Chen, L.; Gong, J.; Osada, Y. *Macromolecules* **1999**, *32*, 3964−3969.
(41) Faïd, K.; Leclerc, M. *J. Am. Chem. Soc.* **1998**, *120*, 5274−5278.
(42) McCullough, R. D.; Ewbank, P. C.; Loewe, R. S. *J. Am. Chem. Soc.* **1997**, *119*, 633−634.
(43) Berggren, M.; Bergman, P.; Fagerstrom, J.; Inganas, O.; Andersson, M.; Weman, H.; Granstrom, M.; Stafstrom, S.; Wennerstrom, O.; Hjertberg, T. *Chem. Phys. Lett.* **1999**, *304*, 84−90.
(44) Nilsson, K. P. R.; Andersson, M. R.; Inganäs, O. *J. Phys.: Condens. Matter* **2002**, *14*, 1−10.

electrolyte chains occurs. This separation of the polyelectrolyte chains is probably due to the interaction between PONT and nBI. Furthermore, in Figure 4, selected spectra from the different phases of the fibril formation process are shown. Upon addition of BI incubated for 4.5 h at 65 °C, a further increase in emission intensity can be seen, signifying a stronger interaction between the insulin and PONT. A major difference in the emission spectrum can be seen after a 6-h incubation of BI. There are two clear emission peaks in the spectrum, the previously observed at 600 nm and a more blue-shifted peak at 560 nm, and the intensity has increased several orders of magnitude. The peak at shorter wavelengths indicates that the polymer backbone adopts a more twisted conformation upon interaction with amyloid fibrils.[9,43] The noteworthy enhancement of the emission intensity suggests that a separation of the oligoelectrolyte chains occur due to the interaction between PONT and fBI. Upon addition of BI heated for 10 h, these phenomena are even more apparent, especially the emission peak at 560 nm, which is increased compared to the peak at 600 nm, and the emission spectrum resembles the spectra seen for PONT in deionized water and at pH 5.9. Hence, the binding of PONT to fBI will induce a more twisted conformation of the oligoelectrolyte backbone and separation of the oligoelectrolyte chains. The optical changes show that the formation of β-sheet-containing amyloid fibrils in fBI are influencing the conformation and the electronic structure of the polyelectrolyte backbone when it binds the fibrils. The geometric alteration of the polyelectrolyte chains might be a result of the conversion, from α-helices to β-sheets, of the secondary structure in the BI molecule. Interestingly, in a similar study with another polymer probe, poly(thiophene acetic acid), PTAA, the formation of amyloid fibrils can be followed, but upon addition of fBI to PTAA, a red shift of the emission maximum is seen.[39]

When PONT is present during amyloid fibril incubation, the changes in emission spectra upon insulin fibril formation have different characteristics (Figure 4). After 10 h of incubation, one clear peak at 585 nm can be seen, indicating that the insulin fibril formation induces a somewhat more twisted conformation of the thiophene backbone compared to PONT in solution (pH 1.6). The increase in emission intensity is a result of separation of the oligomer chains. This blue shift is not a thermochromic phenomenon, since it cannot be seen if the pure oligomer is heated; in fact, if a pure oligomer solution is heated for 10 h, very strong quenching of the fluorescence occurs. The change of emission characteristics and the preservation of the optical properties of the oligomer indicate an incorporation of PONT into the amyloid fibrils. A conjugated polymer integrated in the defined nanostructure of amyloid fibrils is a highly interesting material for the development in self-assembling organic electronics.

To further verify the use of PONT as a conformational-sensitive probe to detect amyloid fibril formation in proteins at acidic pH, experiments with chicken lysozyme were performed (see Supporting Information). Interaction between native chicken lysozyme (nCL) and PONT gives a similar spectrum as the one obtained with nBI (Figure 4 and Supporting Information). Likewise, after addition of 5 μM (on a monomer basis) of amyloid fibrils of lysozyme (fCL) to a PONT solution, the emission spectrum has similar characteristics as the spectrum seen for BI amyloid fibrils (Figure 4 and Supporting Information). The lower emission intensity of the spectrum with fCL compared to the spectrum with nBI is likely due to the large size of the CL fibrils that had been incubated for 220 h, providing lower bulk fluorescence intensity. The fCL spectrum is more blue-shifted and has one well-defined maximum at 550 nm along with shoulders at 520 and 600 nm. These differences can be caused by slightly different amyloid fibril morphology. In comparison to the PONT fluorescence signal bound to amyloid fibrils (fBI or fCL), binding of PONT to collagen type I, which has a native fibril state, showed a spectrum very similar to that of nBI (see Supporting Information, Figure S3), likely due to the intrinsic polyproline type II helical structure of collagen. The similarities in the results obtained with fBI and fCL together with the distinct different spectra of collagen clearly indicate that PONT is a conformation-sensitive probe. Changes of the protein secondary and quaternary structure, associated with the formation of amyloid fibrils, results in conformational changes of the polyelectrolyte backbone upon binding to these structures.

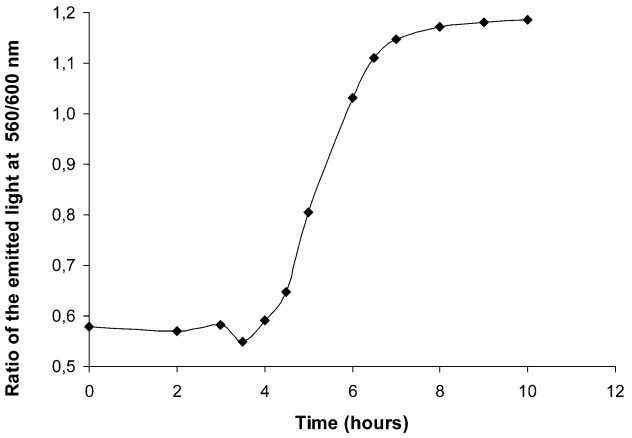

Figure 5. Kinetics of the insulin fibril formation, monitored by PONT fluorescence. The fibril formation was induced by incubation of 320 μM BI at pH 1.6 and 65 °C. An aliquot was withdrawn, and after addition of PONT, the samples were diluted with 25 mM HCl (23 °C) prior to emission measurements.

To perform a spectroscopic evaluation of the different backbone conformations of PONT, induced by the formation of amyloid fibrils of BI, a kinetic study of the formation of amyloid fibrils in BI was carried out. PONT was added after fibrillation, and the emission of the oligoelectrolyte was utilized. The time plot for the formation of amyloid fibrils of BI is shown in Figure 5. By following the ratio of the intensity of the emitted light at 560 and 600 nm, 560/600 nm, the amyloid fibrillation can clearly be monitored by the geometrical alterations in the polymer chains.

An initial lag phase, an exponential growth phase, and a final plateau phase are evident in the graph. The exponential growth phase for amyloid formation occurs during 4−7 h, which is in good agreement with the results obtained from similar experiments using a different polymer.[39] The fluorescence was also recorded for samples incubated for 24 and 72 h, and the ratio of the intensity of the emitted light at 560 and 600 nm was just slightly altered, compared with the sample incubated for 10 h, indicating that the plateau phase for the amyloid formation are reached after 10 h (data not shown). The emission studies agree very well with the results obtained by the TEM studies and the CD measurements. The consistence of these results shows how

the degree of amyloid fibril formation can be monitored with PONT fluorescence.

In the fluorescence spectra and the kinetic studies, it is clearly seen how different states of the amyloid formation can be easily monitored with the oligoelectrolyte. The possibility to detect at low pH used in the amyloid formation process is a noteworthy difference compared to frequently used probes, such as thioflavine T and Congo red.

Conclusions

We have reported the synthesis of a regioregular, zwitterionic, conjugated oligoelectrolyte. Our study shows how this oligoelectrolyte successfully can be used as an optical probe for detection of amyloid fibril formation at low pH. As amyloid fibril formation is a well-known phenomenon associated with several disease conditions, a simple detection system is highly desirable. The method is based on a fast, noncovalent interaction between the protein and the probe. Binding of the oligoelectrolyte to amyloid fibrils results in changes of the geometry and the electronic structure of the oligoelectrolyte chains, which have been monitored with absorption and emission spectroscopy. We suggest that the method described herein can be used for a wide range of proteins, in sensor applications and bioelectronic devices. Furthermore, we have shown indications of the possibility to incorporate the semiconducting oligoelectrolytes into the amyloid fibril structure. The potential of this material lies in the formation of highly ordered, self-assembling elements for organic electronic applications on the nanometer scale.

Acknowledgment. We acknowledge partial funding from VINNOVA and CENANO at LiU (A.H.). Support from the Foundation of Strategic Research (P.H.), the Wenner-Gren Foundations (P.H.), and the Swedish research council (P.H. and J.D.M.O.) are greatly appreciated.

Supporting Information Available: CD spectra of amyloid fibrillation, emission spectra of PONT interacting with chicken lysozyme in native and amyloid fibril form, and emission spectra of PONT interacting with collagen. This material is available free of charge via the Internet at http://pubs.acs.org.

JA045835E